

Measurement of D^0 and D^+ meson masses with the KEDR Detector

V.V. Anashin^a, V.M. Aulchenko^{a,b}, E.M. Baldin^{a,b}, A.K. Barladyan^a, A. Yu. Barnyakov^a, M. Yu. Barnyakov^a, S.E. Baru^{a,b}, I.V. Bedny^a, O.L. Beloborodova^{a,b}, A.E. Blinov^a, V.E. Blinov^{a,c}, A.V. Bobrov^a, V.S. Bobrovnikov^a, A.V. Bogomyagkov^{a,b}, A.E. Bondar^{a,b}, D.V. Bondarev^a, A.R. Buzykaev^a, S.I. Eidelman^{a,b}, Yu.M. Glukhovchenko^a, V.V. Gulevich^a, D.V. Gusev^a, S.E. Karnae^a, G.V. Karpov^a, S.V. Karpov^a, T.A. Kharlamova^{a,b}, V.A. Kiselev^a, S.A. Kononov^{a,b}, K. Yu. Kotov^a, E.A. Kravchenko^{a,b}, V.F. Kulikov^{a,b}, G. Ya. Kurkin^{a,c}, E.A. Kuper^{a,b}, E.B. Levichev^{a,c}, D.A. Maksimov^a, V.M. Malyshev^a, A.L. Maslennikov^a, A.S. Medvedko^{a,b}, O.I. Meshkov^{a,b}, S.I. Mishnev^a, I.I. Morozov^{a,b}, N. Yu. Muchnoi^{a,b}, V.V. Neufeld^a, S.A. Nikitin^a, I.B. Nikolaev^{a,b}, I.N. Okunev^a, A.P. Onuchin^{a,c}, S.B. Oreshkin^a, I.O. Orlov^{a,b}, A.A. Osipov^a, S.V. Peleganchuk^a, S.G. Pivovarov^{a,c}, P.A. Piminov^a, V.V. Petrov^a, A.O. Poluektov^a, I.N. Popkov^a, V.G. Prisekin^a, A.A. Ruban^a, V.K. Sandyrev^a, G.A. Savinov^a, A.G. Shamov^a, D.N. Shatilov^a, B.A. Schwartz^{a,b}, E.A. Simonov^a, S.V. Sinyatkin^a, Yu.I. Skovpen^{a,b}, A.N. Skrinisky^a, V.V. Smaluk^{a,b}, A.V. Sokolov^a, A.M. Sukharev^a, E.V. Starostina^{a,b}, A.A. Talyshev^{a,b}, V.A. Tayursky^a, V.I. Telnov^{a,b}, Yu.A. Tikhonov^{a,b}, K. Yu. Todyshev^{a,b}, G.M. Tumaikin^a, Yu.V. Usov^a, A.I. Vorobiov^a, A.N. Yushkov^a, V.N. Zhilich^a, V.V. Zhulanov^{a,b}, A.N. Zhuravlev^{a,b}

^aBudker Institute of Nuclear Physics, 11, akademika Lavrentieva prospect, Novosibirsk, 630090, Russia

^bNovosibirsk State University, 2, Pirogova street, Novosibirsk, 630090, Russia

^cNovosibirsk State Technical University, 20, Karl Marx prospect, Novosibirsk, 630092, Russia

arXiv:0909.5545v2 [hep-ex] 26 Feb 2010

Abstract

The masses of the neutral and charged D mesons have been measured with the KEDR detector at the VEPP-4M electron-positron collider:

$$M_{D^0} = 1865.30 \pm 0.33 \pm 0.23 \text{ MeV},$$

$$M_{D^+} = 1869.53 \pm 0.49 \pm 0.20 \text{ MeV}.$$

Key words: D meson, charm, mass, $X(3872)$, $\psi(3770)$

PACS: 13.20.Fc, 13.20.Gd, 14.40.Lb

1. Introduction

Neutral and charged D mesons are the ground states in the family of open charm mesons. Measurement of their masses provides a mass scale for the heavier excited states. In addition, a precise measurement of the D^0 meson mass should help to understand the nature of the narrow $X(3872)$ state [1, 2, 3, 4], which, according to some models, is a bound state of D^0 and D^{*0} mesons [5] and has a mass very close to the sum of the D^0 and D^{*0} meson masses. Presently, the world-average D^0 mass value [6] ($M_{D^0} = 1864.84 \pm 0.17 \text{ MeV}$) is dominated by the CLEO measurement $M_{D^0} = 1864.847 \pm 0.150(\text{stat}) \pm 0.095(\text{syst}) \text{ MeV}$ [7], which uses the decay $D^0 \rightarrow \phi K_S^0$. Other D meson mass measurements are much less precise. These measurements were carried out long ago in the MARK-II experiment at the SPEAR e^+e^- collider [8], and by the ACCMOR collaboration in a fixed-target experiment [9]. Both measurements are dominated by the systematic uncertainty, which in the case of MARK-II is related to beam energy calibration. In addition, the mass of the D^+ is constrained by the D^0 mass and a mass difference $M_{D^+} - M_{D^0}$ much more precisely than directly measured: the world-average D^+ mass is $M_{D^+} = 1869.62 \pm 0.20 \text{ MeV}$, while the direct measurements

yield $M_{D^+} = 1869.5 \pm 0.5 \text{ MeV}$.

As both D^0 and D^+ mass values are based on a single measurement, the cross-check involving a method different from the one used at CLEO is essential. This paper describes a measurement which has been performed with the KEDR detector at the VEPP-4M e^+e^- collider using the decay $\psi(3770) \rightarrow D\bar{D}$.

2. Experimental facility

The electron-positron accelerator complex VEPP-4M [10] designed for high-energy physics experiments in the center-of-mass (CM) energy range from 2 to 12 GeV is currently running in the ψ family region. The collider consists of two half-rings, an experimental section where the KEDR detector is installed, and a straight section, which includes an RF cavity and injection system. The circumference of the VEPP-4M ring is 366 m. The luminosity at the J/ψ in an operation mode with 2 by 2 bunches reaches $\mathcal{L} = 10^{30} \text{ cm}^{-2}\text{s}^{-1}$.

Precise measurement of beam energy can be performed at VEPP-4M using the resonant depolarization method [11]. The method is based on the measurement of the spin precession frequency of the polarized beam, which depends on its

energy. Using resonant depolarization, the precision of the beam energy measurement reached in the KEDR experiment is ≈ 10 keV [12].

The KEDR detector [13] includes a tracking system consisting of a vertex detector and a drift chamber, a particle identification (PID) system of aerogel Cherenkov counters and scintillation time-of-flight counters, and an electromagnetic calorimeter based on liquid krypton (in the barrel part) and CsI crystals (endcap part). The superconducting solenoid provides a longitudinal magnetic field of 0.6 T. A muon system is installed inside the magnet yoke. The detector also includes a high-resolution tagging system for studies of two-photon processes. The online luminosity measurement is performed with sampling calorimeters which detect photons from the process of single brehmsstrahlung.

Charged tracks are reconstructed in the drift chamber (DC) and vertex detector (VD). DC [14] has a cylindrical shape of 1100 mm length, an outer radius of 535 mm and is filled with pure dimethyl ether. DC cells form seven concentric layers: four axial layers and three stereo-layers to measure track coordinates along the beam axis. The coordinate resolution averaged over drift length is $100 \mu\text{m}$. VD [15] is installed between the vacuum chamber and DC and increases a solid angle accessible to the tracking system to 98%. VD consists of 312 cylindrical drift tubes aligned in 6 layers. It is filled with an Ar+30%CO₂ gas mixture and has a coordinate resolution of $250 \mu\text{m}$. The momentum resolution of the tracking system is $\sigma_p/p = 2\% \oplus (4\% \times p[\text{GeV}])$.

Scintillation counters of the time-of-flight system (TOF) are used in a fast charged trigger and for identification of the charged particles by their flight time. The TOF system consists of 32 plastic scintillation counters in the barrel part and in each of the endcaps. The flight time resolution is about 350 ps, which corresponds to π/K separation at the level of more than two standard deviations for momenta up to 650 MeV.

Aerogel Cherenkov counters (ACC) [16] are used for particle identification in the momentum region not covered by the TOF system and ionizations measurements in DC. ACC uses aerogel with the refractive index of 1.05 and wavelength shifters for light collection. This allows one to identify π and K mesons in the momentum range of 0.6 to 1.5 GeV. The system design includes 160 counters in the endcap and barrel parts, each arranged in two layers. During data taking only one layer of ACC was installed, and it was not used because of insufficient efficiency.

The barrel part of the electromagnetic calorimeter is a liquid krypton ionization detector [17]. The calorimeter provides an energy resolution of 3.0% at the energy of 1.8 GeV and a spatial resolution of 0.6–1.0 mm for charged particles and photons. The endcap part of the calorimeter is based on 1536 CsI(Na) scintillation crystals [18] with an energy resolution of 3.5% at 1.8 GeV, and a spatial resolution of 8 mm.

The muon system [19] is used to identify muons by their flight path in the dense medium of the magnetic yoke. It consists of three layers of streamer tubes with 74% solid angle coverage, the total number of channels is 544. The average longitudinal resolution is 3.5 cm, and the detection efficiency for the

most of the covered angles is 99%.

Trigger of the KEDR detector consists of two levels: primary (PT) and secondary (ST). Both PT and ST operate at the hardware level. PT uses signals from TOF counters and both calorimeters as inputs, the typical rate is $5 \div 10$ kHz. ST uses signals from VD, DC and muon system in addition to systems listed above, and the rate is $50 \div 150$ Hz.

3. Measurement method

Measurement of D meson masses is performed using the near-threshold $e^+e^- \rightarrow D\bar{D}$ production with full reconstruction of one of the D mesons. Neutral D mesons are reconstructed in the $K^-\pi^+$ final state, charged D mesons are reconstructed in the $K^-\pi^+\pi^+$ final state (charge-conjugate states are implied throughout this paper). To increase a data sample, the collider is operated at the peak of the $\psi(3770)$ resonance. The production cross sections at this energy are $\sigma(D^0\bar{D}^0) = 3.66 \pm 0.03 \pm 0.06$ nb and $\sigma(D^+D^-) = 2.91 \pm 0.03 \pm 0.05$ nb [20].

The invariant mass of the D meson can be calculated as

$$M_{bc} \approx \sqrt{E_{\text{beam}}^2 - \left(\sum_i \vec{p}_i \right)^2}, \quad (1)$$

(so-called *beam-constrained mass*), where E_{beam} is the average energy of colliding beams, \vec{p}_i are the momenta of the D decay products. The mass calculated this way is determined more precisely than in the case when the D energy is obtained from the energies of the decay products. The precision of M_D measurement in one event is

$$\sigma_{M_D}^2 \approx \sigma_W^2/4 + \left(\frac{p_D}{M_D} \right)^2 \sigma_p^2 \approx \sigma_W^2/4 + 0.02\sigma_p^2, \quad (2)$$

where σ_W is the CM energy spread. The contribution of the momentum resolution is suppressed significantly due to small D momentum ($p_D \approx 260$ MeV).

In addition to M_{bc} , D mesons are effectively selected by the CM energy difference

$$\Delta E = \sum_i \sqrt{M_i^2 + p_i^2} - E_{\text{beam}}, \quad (3)$$

where M_i and p_i are the masses and momenta of the D decay products. The signal events should satisfy a condition $\Delta E \approx 0$. In our analysis, we select a relatively wide region of M_{bc} and ΔE close to $M_{bc} \sim M_D$ and $\Delta E \sim 0$ (specifically, $M_{bc} > 1700$ MeV, $|\Delta E| < 300$ MeV); then a fit of the event density is performed with D mass as one of the parameters, with the background contribution taken into account. The background in our analysis comes from the random combinations of tracks of the continuum process $e^+e^- \rightarrow q\bar{q}$ ($q = u, d, s$), from other decays of D mesons, and from the signal decays where some tracks are picked up from the decay of the other D meson.

While calculating M_{bc} , we employ a kinematic fit with the $\Delta E = 0$ constraint. It is done by minimizing the χ^2 function

formed by the momenta of the daughter particles

$$\chi^2 = \sum_i \frac{(p'_i - p_i)^2}{\sigma_{p_i}^2}, \quad (4)$$

where p_i and σ_{p_i} are the measured momenta of the daughter particles and their errors obtained from the track fit, respectively, and p'_i are the fitted momenta which satisfy the $\Delta E(p'_i) = 0$ constraint. The use of M_{bc} constructed from the fitted momenta results in a certain improvement of its resolution and significantly reduces the dependence of measured mass on the absolute momentum calibration (see below).

The precision of the momentum measurement has direct influence on the D mass measurement. The following sources of momentum reconstruction uncertainties are considered in our analysis:

1. Simulation of ionization losses in the detector material.

Reconstruction of cosmic tracks is used to check the validity of the simulation. We select the cosmic tracks that traverse the vacuum chamber and fit their upper and lower parts separately. The average difference of the upper and the lower track momenta due to energy loss in the detector material is compared with the result of the simulation.

2. **Absolute momentum calibration** (this is equivalent to the knowledge of the average magnetic field in the tracking system), described by the scale coefficient α which relates the true track momentum p_{true} and the measured momentum p :

$$p_{\text{true}} = \alpha p. \quad (5)$$

Then

$$M_D = \sqrt{E_{\text{beam}}^2 - \alpha^2 \left(\sum_i \vec{p}_i \right)^2}, \quad (6)$$

$$\frac{dM_D}{d\alpha} \simeq -\frac{p_D^2}{M_D} \simeq -36 \text{ MeV}. \quad (7)$$

The momentum scale can be calibrated using the same events as in the D mass measurement by measuring the average bias of the ΔE value:

$$\Delta E = \sum_i \sqrt{M_i^2 + \alpha^2 p_i^2} - E_{\text{beam}}. \quad (8)$$

Sensitivities to the scale coefficient α are given by

$$\frac{d\Delta E}{d\alpha} \simeq \frac{p_K^2}{E_K} + \frac{p_\pi^2}{E_\pi} \simeq 1580 \text{ MeV} \quad (9)$$

for $D^0 \rightarrow K^- \pi^+$ decay, and

$$\frac{d\Delta E}{d\alpha} \simeq 1490 \text{ MeV} \quad (10)$$

for $D^+ \rightarrow K^- \pi^+ \pi^+$ decay. The numerical values of the $d\Delta E/d\alpha$ derivatives are obtained using the Monte Carlo (MC) simulation of the corresponding decays. When the kinematic fit with $\Delta E = 0$ is employed for an M_{bc} calculation, such a correction is effectively applied to

each event, and thus the dependence of M_D on the absolute momentum calibration is significantly reduced (to $dM_D/d\alpha = -3 \text{ MeV}$ for $D^0 \rightarrow K^- \pi^+$ and -12 MeV for $D^+ \rightarrow K^- \pi^+ \pi^+$).

As a cross-check, we also use other processes for the absolute momentum calibration: the inclusive $K_S^0 \rightarrow \pi^+ \pi^-$ reconstruction and $e^+ e^- \rightarrow \psi(2S) \rightarrow J/\psi \pi^+ \pi^-$ process.

3. **Simulation of the momentum resolution.** Since the D meson sample is limited, we use full MC simulation of the detector to determine the shapes of the signal distributions. The description of the momentum resolution in the simulation is adjusted using events of elastic $e^+ e^-$ scattering, inclusive reconstruction of $K_S^0 \rightarrow \pi^+ \pi^-$ decay, and the process $e^+ e^- \rightarrow \psi(2S) \rightarrow J/\psi \pi^+ \pi^-$.

4. Analysis of $D^0 \rightarrow K^- \pi^+$

The analysis uses a sample of 0.9 pb^{-1} accumulated with the KEDR detector at the energy of the $\psi(3770)$ resonance. Multihadron candidates which contain at least three tracks close to the interaction region (transverse distance from the beam $R < 5 \text{ mm}$, and longitudinal distance $|z| < 120 \text{ mm}$) forming a common vertex are selected at the first stage of the analysis. The pairs of oppositely charged tracks are taken as D^0 decay candidates with the following requirements:

- Number of track hits $N_{\text{hits}} \geq 24$ (the maximum number of hits per track is 48),
- Track fit quality $\chi^2/ndf < 50$,
- Transverse momentum: $100 \text{ MeV} < p_T < 2000 \text{ MeV}$.
- Energy of the associated cluster in the calorimeter $E < 1000 \text{ MeV}$.

We expect around 100 $D^0 \rightarrow K^- \pi^+$ signal events for this sample. In order to measure the D^0 mass most efficiently, the unbinned maximum likelihood fit procedure is used. Except for the M_{bc} variable, the likelihood function includes two other variables which allow one to efficiently separate the signal from the background: the energy difference $\Delta E = E_D - E_{\text{beam}}$ (8) and the difference of the absolute values of momenta for D decay products in the CM frame $\Delta|p|$.

The likelihood function has the form:

$$-2 \log \mathcal{L}(\alpha) = -2 \sum_{i=0}^N \log p(\mathbf{v}_i|\alpha) + 2N \log \int p(\mathbf{v}|\alpha) d\mathbf{v}, \quad (11)$$

where $\mathbf{v} = (M_{bc}, \Delta E, \Delta|p|)$ are the variables that characterize one event, $p(\mathbf{v}|\alpha)$ is the probability distribution function (PDF) of these variables depending on the fit parameters $\alpha = (M_D, \langle \Delta E \rangle, b_{uds}, b_{DD})$:

$$p(\mathbf{v}|\alpha) = p_{\text{sig}}(\mathbf{v}|M_D, \langle \Delta E \rangle) + b_{uds} p_{uds}(\mathbf{v}) + b_{DD} p_{DD}(\mathbf{v}). \quad (12)$$

Here p_{sig} is the PDF of the signal events which depends on M_D (D^0 mass) and $\langle \Delta E \rangle$ (the central value of the ΔE distribution), p_{uds} is the PDF for the background process $e^+ e^- \rightarrow q\bar{q}$

($q = u, d, s$), and p_{DD} is the PDF for the background from $e^+e^- \rightarrow D\bar{D}$ decays with D decaying to all modes other than the signal one, b_{uds} and b_{DD} are their relative magnitudes. The shape of the p_{sig} , p_{uds} and p_{DD} distributions is obtained from the MC simulation. Such a fit procedure gives only a shape of the fitted distribution without the absolute normalization. The numbers of signal and background events can be extracted by taking the total number of events in a sample and fractions of the corresponding events from the fit.

For a proper calculation of $\Delta E = E_\pi + E_K - E_{beam}$, the π/K identification is needed. Presently it cannot be performed reliably in the momentum range near 800 MeV. Fortunately, since the D meson momentum is small, the momenta of K and π differ by a small amount, and the maximum error (in the case of wrong mass assignment) is not larger than 30 MeV. Thus, we take the following combination as a D meson energy:

$$E' = (E_{K^-\pi^+} + E_{K^+\pi^-})/2, \quad (13)$$

where

$$\begin{aligned} E_{K^-\pi^+} &= \sqrt{M_K^2 + p_-^2} + \sqrt{M_\pi^2 + p_+^2}, \\ E_{K^+\pi^-} &= \sqrt{M_K^2 + p_+^2} + \sqrt{M_\pi^2 + p_-^2}. \end{aligned} \quad (14)$$

The energy E' calculated this way is practically unbiased from the true energy E . A bias can appear if the detection efficiency varies with momenta of the final state particles; we estimate the upper limit of this bias to be 1.5 MeV. According to (7) and (9), this bias is propagated to an M_{D^0} bias of 0.034 MeV. E' differs from E by less than 15 MeV in each event, this only slightly affects the ΔE error due to momentum resolution.

Use of the $\Delta|p|$ variable allows us to obtain an estimate of the M_{bc} resolution on the event-by-event basis, thus improving the overall statistical accuracy of the measurement. We use the fact that this resolution depends strongly on decay kinematics — it can be up to three times better for events where the daughter particles from D^0 decay move transversely to the direction of the D^0 ($\Delta|p|$ is around zero for these events), than for events where they move along this direction (see Fig. 1).

The variables M_{bc} and $\Delta|p|$ use the momenta of the daughter particles after the kinematic fit with the $\Delta E = 0$ constraint, while ΔE is calculated using uncorrected momenta. We select combinations that satisfy the following requirements for the further analysis: $M_{bc} > 1700$ MeV, $|\Delta E| < 300$ MeV.

Simulation of signal events is performed with the MC generator for $e^+e^- \rightarrow D\bar{D}$ decays where D -meson decays are simulated by the JETSET 7.4 package [21], and the radiative corrections are taken into account in both initial (ISR, using the RADCOR package [22] with Kuraev-Fadin model [23]), and final states (FSR, the PHOTOS package [24]). The ISR corrections use the $e^+e^- \rightarrow D\bar{D}$ cross section dependence of the resonant production of the $\psi(3770)$ according to a Breit-Wigner amplitude with $M = 3771$ MeV and $\Gamma = 23$ MeV [25], without the nonresonant contribution and taking into account phase space dependence at the production threshold. The full simulation of the KEDR detector is performed using the GEANT 3.21 package [26].

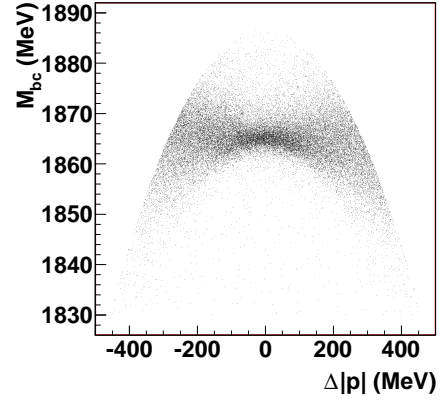


Figure 1: Correlation of M_{bc} and $\Delta|p|$ variables for $D^0 \rightarrow K^-\pi^+$ decays (MC simulation).

The PDF of the signal events p_{sig} is a function of three parameters M_{bc} , ΔE , and $\Delta|p|$. It is parameterized with the sum of two two-dimensional Gaussian distributions in M_{bc} and ΔE (representing the core and the tails of the distribution) with a correlation and with the quadratic dependence of the M_{bc} resolution on $\Delta|p|$. The core distribution is asymmetric in M_{bc} (with the resolutions $\sigma_L(M_{bc})$ and $\sigma_R(M_{bc})$ for the left and right slopes, respectively). The $\Delta|p|$ distribution is uniform with a small quadratic correction and with the kinematic constraint $(\Delta|p|)^2 < E_{beam}^2 - M_{bc}^2$. The parameters of the signal distribution are obtained from the fit to the simulated signal sample. The core resolutions obtained from the MC for M_{bc} are $\sigma_L(M_{bc}) = 0.98 \pm 0.03$ MeV, $\sigma_R(M_{bc}) = 2.45 \pm 0.06$ MeV (at $\Delta|p| = 0$), the M_{bc} resolution at $\Delta|p| = 200$ MeV is 4.6 ± 0.1 MeV, the core resolution of ΔE is 48.3 ± 0.3 MeV.

The background from the continuum $e^+e^- \rightarrow q\bar{q}$ process (where $q = u, d, s$) is simulated using the JETSET 7.4 $e^+e^- \rightarrow q\bar{q}$ generator. The PDF is parameterized as

$$p_{uds}(M_{bc}, \Delta E, \Delta|p|) = \exp\left(-k_1 \left[1 - \frac{M_{bc}^2}{E_{beam}^2}\right] - k_2 \Delta E\right) \times (1 + k_3 \Delta|p|^2), \quad (15)$$

where k_i are free parameters. The kinematic limit at $M_{bc} = E_{beam}$ is provided by the $(\Delta|p|)^2 < E_{beam}^2 - M_{bc}^2$ constraint.

The background from $e^+e^- \rightarrow D\bar{D}$ decays is simulated using the JETSET 7.4 generator, where the signal process $D^0 \rightarrow K^-\pi^+$ is suppressed in the decay table. The PDF for $D\bar{D}$ background is parameterized with the function p_{DD} of the same form as for p_{uds} , with the addition of three two-dimensional Gaussian distributions in M_{bc} and ΔE . Two of them describe the background from $D^0 \rightarrow \pi^+\pi^-$ and $D^0 \rightarrow K^+K^-$, while the third one is responsible for the decays of D mesons to three and more particles.

The combinatorial background coming from the signal events where one or more tracks were taken from the decay of the other D meson, were studied using the signal MC sample. The distribution of fit variables for these events is similar to the background from the continuum events, and their fraction is

Table 1: Results of the fit to the $D^0 \rightarrow K^- \pi^+$ data sample

M_D	1865.05 ± 0.33 MeV
$\langle \Delta E \rangle$	-0.7 ± 7.3 MeV
Number of signal events	98.4 ± 13.1
Number of $q\bar{q}$ events	18.3 ± 2.4
Number of $D\bar{D}$ events	4.8 ± 0.8

2.5% of the number of signal events, which is negligible compared to the continuum contribution. We therefore do not treat this background separately, and its contribution is effectively taken by the continuum component.

The result of the fit to the experimental data is shown in Fig. 2. In the fit we use the function (12) with M_D , $\langle \Delta E \rangle$ as well as the relative magnitudes of the continuum and $D\bar{D}$ backgrounds as free parameters.

The momentum correction coefficient α is chosen to keep the value of $\langle \Delta E \rangle$ close to zero. Event selection is performed with $\alpha = 1.030$; after the residual ΔE bias is taken into account its value is $\alpha = 1.0304 \pm 0.0046$. The results of the fit are shown in Table 1. The numbers of events are presented for the signal region $|\Delta E| < 100$ MeV, 1855 MeV $< M_{bc} < 1875$ MeV.

To obtain the D^0 mass, one has to take into account a possible deviation of the fit parameters M_D and $\langle \Delta E \rangle$ from the true D^0 mass and energy. In particular, the central value of M_D can be shifted due to the asymmetric resolution function and radiative corrections. This deviation is corrected using the MC simulation. The final value of the D^0 mass after the correction is $M_{D^0} = 1865.30 \pm 0.33$ MeV.

5. Analysis of $D^+ \rightarrow K^- \pi^+ \pi^+$

The three-body decay $D^+ \rightarrow K^- \pi^+ \pi^+$ has more kinematic parameters and there is no simple variable (such as $\Delta|p|$ in the $D^0 \rightarrow K^- \pi^+$ case), which determines the precision of the M_{bc} reconstruction. Therefore, we use only two variables, M_{bc} and ΔE , in a fit of this mode.

The mode $D^+ \rightarrow K^- \pi^+ \pi^+$ does not have a problem with π/K identification for the ΔE calculation, since the sign of the kaon charge is opposite to the pion charges and thus energies of all the particles can be obtained unambiguously. The triplets of tracks with the charge of one of the tracks ("kaon") opposite to the charges of the two other tracks ("pions") are taken as D^\pm decay candidates.

The requirements for the track selection are the same as in the $D^0 \rightarrow K^- \pi^+$ case. Since the significant part of the kaon tracks in the three-body decay have relatively low momentum (under 500 MeV), an additional suppression of the background from pions is possible using the TOF system. The selection uses the following requirement on the flight time for a kaon candidate, which hits the barrel part of the TOF system: $\Delta T_{TOF} = T_{TOF} - T_K(p_K) > -0.8$ ns (or 2.3 times the flight time resolution), where $T_K(p_K)$ is the expected flight time for a kaon with the momentum p_K and T_{TOF} is the measured flight time. As a result of this requirement the background fraction

Table 2: Results of the fit to the $D^+ \rightarrow K^- \pi^+ \pi^+$ data sample

M_D	1869.58 ± 0.49 MeV
$\langle \Delta E \rangle$	2.5 ± 5.0 MeV
Number of signal events	109.8 ± 15.3
Number of $q\bar{q}$ events	85.3 ± 11.8
Number of $D\bar{D}$ events	11.4 ± 2.2

is reduced by a factor of 2.3 for the continuum background and 3.3 for the $D\bar{D}$ background.

The M_{bc} variable uses the momenta of the daughter particles after the kinematic fit with the $\Delta E = 0$ constraint. The variable ΔE is calculated using uncorrected momenta. We select combinations that satisfy the following requirements for the further analysis: $M_{bc} > 1700$ MeV, $|\Delta E| < 300$ MeV.

As in the case of $D^0 \rightarrow K^- \pi^+$ decay, simulation is performed using the $e^+e^- \rightarrow D\bar{D}$ generator taking into account the ISR and FSR effects. The signal PDF p_{sig} is parameterized in the same way as for the $D^0 \rightarrow K^- \pi^+$ mode, but without $\Delta|p|$ dependence. The core resolutions obtained from the MC for M_{bc} are $\sigma_L(M_{bc}) = 2.07 \pm 0.05$ MeV, $\sigma_R(M_{bc}) = 2.52 \pm 0.06$ MeV, the core resolution of ΔE is 26.5 ± 0.4 MeV.

To parameterize the continuum $e^+e^- \rightarrow q\bar{q}$ background, we use the empirical function of M_{bc} proposed in the Argus experiment [27] and the exponent of the quadratic form in ΔE :

$$p_{uds}(M_{bc}, \Delta E) = y \exp\left(-k_1 y^2 - [k_2 + k_3 y^2] \Delta E + k_4 \Delta E^2\right), \quad (16)$$

where $y = \sqrt{1 - M_{bc}^2/E_{beam}^2}$. The coefficients k_i are free parameters in the fit. The coefficient k_3 is responsible for the M_{bc} dependence of the ΔE slope, which appears after the kinematic fit to $\Delta E = 0$. The PDF for the $e^+e^- \rightarrow D\bar{D}$ background p_{DD} is parameterized with the distribution of the same form as for p_{uds} , with the addition of two two-dimensional Gaussian distributions in M_{bc} and ΔE . They describe the contributions of $D^+ \rightarrow K^+ K^- \pi^+$ and D decays to four and more particles. The combinatorial background from the signal events as in the case of the $D^0 \rightarrow K^- \pi^+$ mode is effectively taken into account by the continuum component.

The result of the fit to the data is shown in Fig. 3. The momentum correction factor α is chosen such that $\langle \Delta E \rangle$ is close to zero. The value $\alpha = 1.027$ is used for event selection, and after taking into account the residual ΔE bias its value is $\alpha = 1.0252 \pm 0.0035$. The results of the fit are shown in Table 2. The numbers of events are shown for the signal region $|\Delta E| < 70$ MeV, 1860 MeV $< M_{bc} < 1880$ MeV.

As in the case of the $D^0 \rightarrow K^- \pi^+$ mode, the D^+ mass obtained in the fit is corrected for the bias of M_D and ΔE using MC simulation. The value of the D^+ mass after the correction is $M_{D^+} = 1869.53 \pm 0.49$ MeV.

6. Systematic uncertainties

The estimates of systematic uncertainties in the D mass measurements are shown in Table 3.

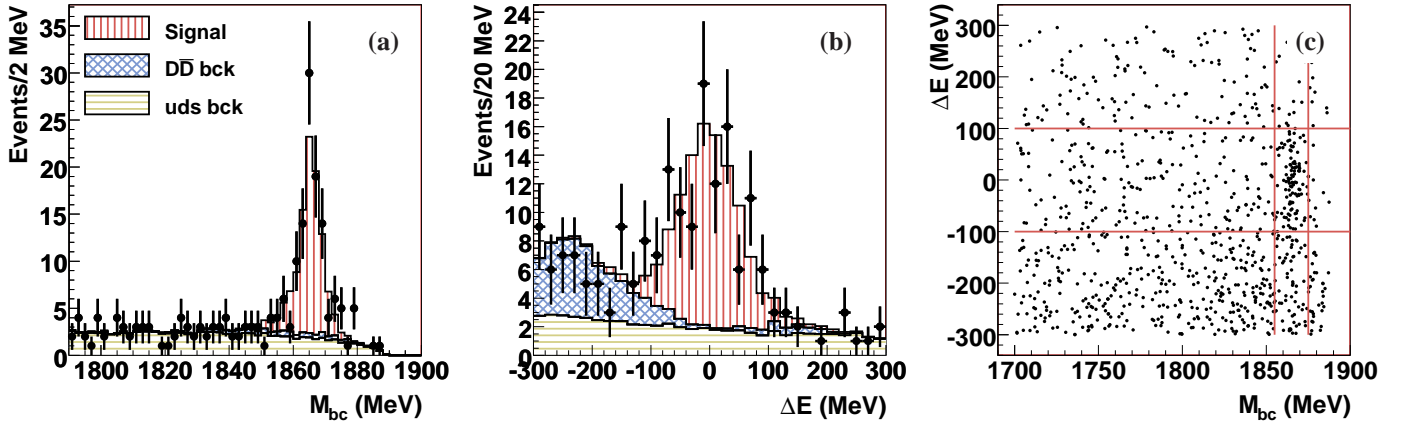


Figure 2: Experimental data (points with the error bars) and the results of the fit (histogram) for the $D^0 \rightarrow K^- \pi^+$ decay. M_{bc} distribution for events with $|\Delta E| < 100$ MeV (a), ΔE distribution for events with $1855 \text{ MeV} < M_{bc} < 1875 \text{ MeV}$ (b), and the experimental $(M_{bc}, \Delta E)$ scatter plot (c).

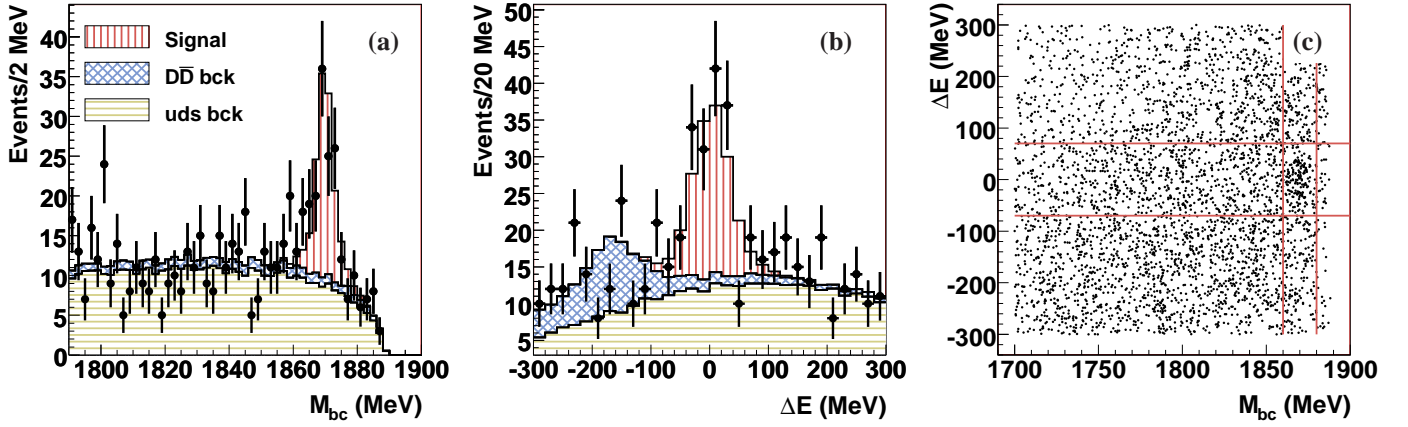


Figure 3: Experimental data (points with the error bars) and the results of the fit (histogram) for the $D^+ \rightarrow K^- \pi^+ \pi^+$ decay. M_{bc} distribution for events with $|\Delta E| < 70$ MeV (a), ΔE distribution for events with $1860 \text{ MeV} < M_{bc} < 1880 \text{ MeV}$ (b), and the experimental $(M_{bc}, \Delta E)$ scatter plot (c).

Table 3: Systematic uncertainties in the D^0 and D^+ mass measurements

	ΔM_{D^0} , MeV	ΔM_{D^+} , MeV
Absolute momentum calibration	0.04	0.04
Ionization loss in material	0.01	0.03
Momentum resolution	0.13	0.10
ISR corrections	0.16	0.11
Signal PDF	0.07	0.05
Continuum background PDF	0.04	0.09
$D\bar{D}$ background PDF	0.03	0.06
Beam energy calibration	0.01	0.01
Total	0.23	0.20

The contribution of absolute momentum calibration is determined by the precision of the $\langle \Delta E \rangle$ measurement and is propagated to the uncertainty of the mass measurement using the $dM_{bc}/d\alpha$ dependence. For the $D^0 \rightarrow K^- \pi^+$ mode, the additional factor, which dominates the momentum calibration error, is a possible bias of the approximate D energy calculation using Eq. (13) in the absence of π/K identification. However, due to smaller $dM_{bc}/d\alpha$ value the momentum calibration uncertainty for this mode is close to the one for the $D^+ \rightarrow K^- \pi^+ \pi^+$ mode.

The uncertainty of the simulation of ionization losses in the detector material is estimated by the variation of the corresponding correction term within the limits given by the cosmic track measurement ($\pm 20\%$).

The uncertainty due to momentum resolution is estimated by using different procedures matching the resolution in the simulation with the experimental one (either by introducing a correction to the drift curve of the DC, or by smearing the reconstructed momenta) and by varying the tuning parameters responsible for the momentum resolution matching within the limits given by the calibration processes.

The ISR correction uncertainty is dominated by the uncer-

tainty of the energy dependence of the cross section $\sigma(e^+e^- \rightarrow D\bar{D})$. The default fit uses the $\psi(3770)$ parameters from PDG-2006 for the cross section ($M = 3771.1 \pm 2.4$ MeV and $\Gamma = 23.0 \pm 2.7$ MeV [25]). To estimate a systematic error, these parameters are varied within their errors, also the PDG-2008 value is used ($\Gamma = 27$ MeV [6]). In addition, the nonresonant contribution is added incoherently to the 1 nb cross section at the $\psi(3770)$ peak. The quadratic sum of deviations in M , Γ and non-resonant contribution is taken as the systematic error. The model uncertainty of Kuraev-Fadin formulae [23] is small ($\sim 0.1\%$) and has a negligible effect on our results.

The uncertainty due to signal shape parameterization is estimated by using the alternative shape with one Gaussian peak.

The continuum background shape uncertainty is estimated by using the alternative generator for the system of pions with the varying multiplicity in the simulation, and also by relaxing the background shape parameters in the experimental fit. The contribution of the DD background shape is estimated by relaxing the relative magnitude of the Gaussian peaks and the non-peaking component in the experimental fit, and by excluding one of the Gaussian peaks from the background shape parameterization. In the case of the $D^+ \rightarrow K^-\pi^+\pi^+$ mode, the background shape variation also includes the shapes obtained without a TOF requirement to take into account the uncertainty in the TOF simulation.

To check possible inconsistencies in the three-dimensional signal and background description of the $D^0 \rightarrow K^-\pi^+$ mode, we perform separate fits to data with different $\Delta|p|$ requirements. The results are consistent within statistical errors.

The error of the beam energy calibration is dominated by the precision of the beam energy interpolation between successive energy measurements using the resonant depolarization technique. It does not exceed 70 keV and is of order 10 keV for most of the data sample. The uncertainty due to beam energy calibration is estimated in the worst case of a 100% correlation between all energy measurements.

7. Conclusion

Masses of the neutral and charged D mesons have been measured with the KEDR detector at the VEPP-4M e^+e^- collider operated in the region of the $\psi(3770)$ meson. The analysis uses a data sample of 0.9 pb^{-1} with D mesons reconstructed in the decays $D^0 \rightarrow K^-\pi^+$ and $D^+ \rightarrow K^-\pi^+\pi^+$. The values of the masses obtained are

- $M_{D^0} = 1865.30 \pm 0.33 \pm 0.23$ MeV,
- $M_{D^+} = 1869.53 \pm 0.49 \pm 0.20$ MeV.

The D^0 mass value is consistent with the more precise measurement of the CLEO collaboration [7], while that of the D^+ mass is presently the most precise direct determination.

Comparison of the D meson masses obtained in this analysis with the other measurements is shown in Fig. 4.

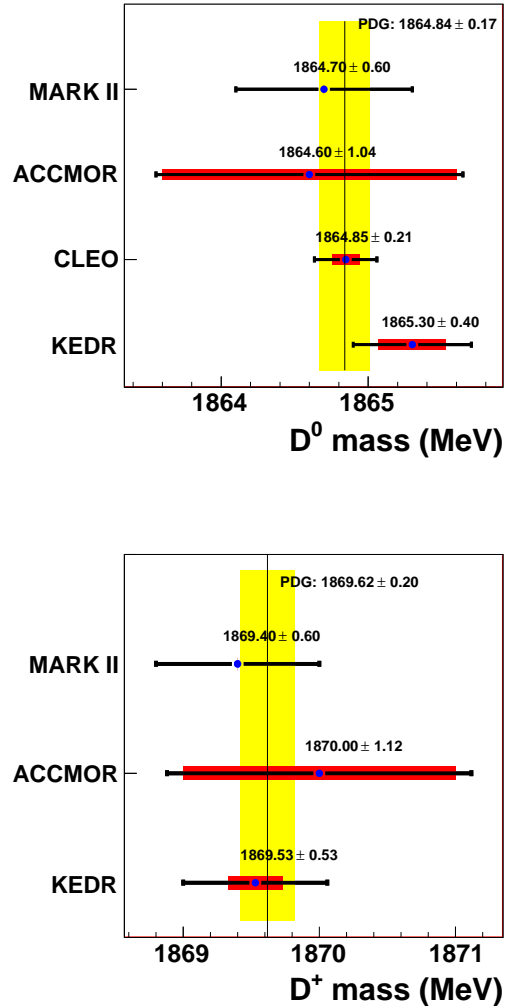


Figure 4: Comparison of D meson masses with the other measurements. The thick and thin error bars show the systematic and the total errors, respectively. The shaded areas are the PDG-2008 values [6]. The PDG value for the D^+ is obtained using the measured mass difference of the D^+ and D^0 mesons. MARK-II does not quote the systematic error separately.

8. Acknowledgments

We are grateful to the BINP administration for the permanent interest to this study and support of KEDR and VEPP-4M operation. This work is partially funded by Russian Foundation for Basic Research, grants 04-02-16712-a and 07-02-01162-a.

References

- [1] Belle Collaboration, S. K. Choi *et al.*, Phys. Rev. Lett. **91**, 262001 (2003).
- [2] CDF Collaboration, D. E. Acosta *et al.*, Phys. Rev. Lett. **93**, 072001 (2004).
- [3] D0 Collaboration, V. M. Abazov *et al.*, Phys. Rev. Lett. **93**, 162002 (2004).
- [4] BaBar Collaboration, B. Aubert *et al.*, Phys. Rev. D **71**, 071103 (2005).
- [5] E. S. Swanson, Phys. Lett. B **588**, 189 (2004).
- [6] Particle Data Group, C. Amsler *et al.*, Phys. Lett. B **667**, 1 (2008).

- [7] CLEO Collaboration, C. Cawfield *et al.*, Phys. Rev. Lett. **98**, 092002 (2007).
- [8] MARK-II collaboration, R. H. Schindler *et al.*, Phys. Rev. D **24**, 78 (1981).
- [9] ACCMOR Collaboration, S. Barlag *et al.*, Z. Phys. C **46**, 563 (1990).
- [10] V. Anashin *et al.*, Stockholm 1998, EPAC 98*, 400 (1998), Prepared for 6th European Particle Accelerator Conference (EPAC 98), Stockholm, Sweden, 22-26 Jun 1998.
- [11] A. N. Skrinsky and Y. M. Shatunov, Sov. Phys. Usp. **32**, 548 (1989).
- [12] KEDR Collaboration, V. M. Aulchenko *et al.*, Phys. Lett. B **573**, 63 (2003).
- [13] V. V. Anashin *et al.*, Nucl. Instrum. Meth. A **478**, 420 (2002).
- [14] S. E. Baru *et al.*, Nucl. Instrum. Meth. A **494**, 251 (2002).
- [15] V. M. Aulchenko *et al.*, Nucl. Instrum. Meth. A **283**, 528 (1989).
- [16] A. Y. Barnyakov *et al.*, Nucl. Instrum. Meth. A **494**, 424 (2002).
- [17] S. Peleganchuk, Nucl. Instr. and Meth. A **598**, 248 (2009).
- [18] V. M. Aulchenko *et al.*, Nucl. Instrum. Meth. A **379**, 502 (1996).
- [19] V. M. Aulchenko *et al.*, Nucl. Instrum. Meth. A **265**, 137 (1988).
- [20] CLEO Collaboration, S. Dobbs *et al.*, Phys. Rev. D **76**, 112001 (2007).
- [21] T. Sjostrand and M. Bengtsson, Comput. Phys. Commun. **43**, 367 (1987).
- [22] S. E. Avvakumov *et al.*, (2006), BINP preprint 2006-038 (in Russian).
- [23] E. A. Kuraev and V. S. Fadin, Sov. J. Nucl. Phys. **41**, 466 (1985).
- [24] E. Barberio and Z. Was, Comput. Phys. Commun. **79**, 291 (1994).
- [25] W.-M. Yao *et al.*, Journal of Physics G **33**, 1 (2006).
- [26] R. Brun *et al.*, CERN Report No. DD/EE/84-1 (1993).
- [27] ARGUS Collaboration, H. Albrecht *et al.*, Phys. Lett. B **241**, 278 (1990).